Environmental Science Nano

PAPER

View Article Online
View Journal | View Issue

Cite this: *Environ. Sci.: Nano*, 2016, 3, 127

Interaction between palladium-doped zerovalent iron nanoparticles and biofilm in granular porous media: characterization, transport and viability†

Mohan Basnet,[a] Alexander Gershanov,[a] Kevin J. Wilkinson,[b] Subhasis Ghoshal[c] and Nathalie Tufenkji*[a]

Received 23rd May 2015,
Accepted 23rd October 2015

DOI: 10.1039/c5en00109a

rsc.li/es-nano

Palladium-doped nanoscale zerovalent iron (Pd-NZVI) can induce rapid transformations of a variety of pollutants during *in situ* remediation of contaminated aquifers. Pd-NZVI stabilized with polymeric surface modifiers has shown substantially improved stability and transport compared to bare Pd-NZVI in model subsurface granular media such as clean quartz sand. The natural subsurface environment is, however, much more complex. For example, biofilms may coat aquifer grain surfaces and thus alter the transport of these reactive nanoparticles. Herein, we compare the transport behavior of Pd-NZVI coated with carboxymethylcellulose or rhamnolipid as surface modifiers, in clean and biofilm-coated sand packed columns. Transport studies suggest that, for both types of nanoparticles tested, the particle attachment efficiency to the collector surface generally increases (up to 6 fold in NaCl and 26 fold in $CaCl_2$) in the presence of biofilm. This result indicates the potential for reduced Pd-NZVI transport in a natural groundwater system. The retentive behavior of biofilm-coated media increases with particle–particle aggregation (*e.g.*, C/C_0 ~ 0.15 for a markedly aggregated CMC-coated Pd-NZVI in divalent salt), implicating physical straining as an important retention mechanism. Retained Pd-NZVI on biofilm-laden matrices was characterized using enhanced darkfield hyperspectral imaging. Assessments of biofilm viability imply that the retained surface-modified Pd-NZVI is non-toxic to the cells within the biofilm matrices (viability >95%). Moreover, the coating molecules do not negatively impact the viability of the biofilm bacteria.

Nano impact

The success of Pd-NZVI based site remediation depends on the mobility of injected Pd-NZVI to reach the target contaminants. The mobility of Pd-NZVI is shown to be reduced in the presence of biofilm on the surface of aquifer grains. The retained surface-modified Pd-NZVI is shown to be generally non-toxic to the biofilm cells and enhanced darkfield hyperspectral imaging is used for identification of Pd-NZVI retention on the biofilm-coated sand. Overall, this study emphasizes that the influence of biofilm should be taken into account when predicting the fate and transport of reactive nanoparticles in the aquatic environment. Thus, our results have implications for the successful implementation of nanotechnology enabled soil and groundwater remediation.

Introduction

Palladium-doped nanoscale zerovalent iron (Pd-NZVI) has been shown to remediate a wide range of contaminants.[1–3] Direct injection has been suggested as a viable method to deliver these reactive nanoparticles to contaminated subsurface zones.[2,4] A major challenge in implementing this technology is that bare Pd-NZVI rapidly aggregates and thus exhibits negligible transport whereas the success of nanotechnology enabled remediation largely depends on the mobility of injected Pd-NZVI to reach the targeted contaminants. Several studies have demonstrated that surface modification of the nanoparticles reduces aggregation and concurrently enhances transport.[5–8] However, these studies were based on mobility experiments conducted in a clean sand-

[a] *Department of Chemical Engineering, McGill University, Montreal, Quebec H3A 0C5, Canada. E-mail: nathalie.tufenkji@mcgill.ca; Fax: +(514) 398 6678; Tel: +(514) 398 2999*
[b] *Department of Chemistry, University of Montreal, Montreal, Quebec H3C 3J7, Canada*
[c] *Department of Civil Engineering, McGill University, Montreal, Quebec H3A 0C3, Canada*

† Electronic supplementary information (ESI) available: Biomass distribution along the column, Pd-NZVI characterizations (EPM and sizing), column breakthrough curves, a summary table for column experiments (C/C_0 values), a summary table for measured influent and effluent DLS sizes, hyperspectral imaging for Pd-NZVI suspension, and Live/Dead microscopy images. See DOI: 10.1039/c5en00109a

packed medium;[5–9] other studies have assessed NZVI mobility in the presence of ions,[5,7] shear-thinning fluids[10] and natural organic matter.[11] The natural subsurface environment, however, is not clean and sterile but contains microbes that have the ability to form biofilms on aquifer grain surfaces that could presumably alter the fate of these reactive nanoparticles. Yet, the transport behavior of Pd-NZVI, in the presence of bacteria or biofilms has not been examined.

There is a growing interest in the investigation of nanoparticle mobility in the presence of biofilm on aquifer grain surfaces. The key features of such studies include (i) the choice of nanoparticles (ZnO,[12] CeO_2,[13] TiO_2,[13] Ag,[13,14] C_{60},[15] quantum dots,[16] polystyrene latex[16] and NZVI[17]), (ii) the choice of biofilm forming bacteria (*P. aeruginosa*[14,17] and *E. coli*[12,15]), (iii) the choice of collector surface to grow the biofilm (quartz sand[12,14,15] and glass beads[17]), and (iv) growth methods (biofilm grown in the seeded column[12,15,17,18] in a circulation mode *versus* biofilm grown in a batch culture[14]) (Table S1†). In nearly all studies, the general conclusion is that the presence of biofilm attenuates nanoparticle mobility (*i.e.*, increases nanoparticle retention in the presence of biofilm) compared to systems without biofilms.[19] In contrast, two studies report lower nanoparticle (PVP-*n*Ag) retention in the presence of biofilm and attribute this observation to electrosteric repulsion between the PVP coating and bacterial extracellular polymeric substances (EPS).[14,18] A study that examined NZVI transport in a column packed with biofilm-coated glass beads reported reduced transport in the presence of biofilm at 25 mM NaCl but no changes in particle transport behavior at lower ionic strength (1 mM NaCl).[17] Because nanoparticle mobility is crucial for the successful implementation of NZVI-based site remediation, it is of interest to conduct a more systematic study of reactive Pd-NZVI transport under a wider range of electrolyte compositions representative of common groundwaters. For example, the influence of divalent salts present in groundwater on particle surface charge and particle aggregation state is well documented in several studies.[5,20–22] For the successful implementation of nanotechnology-enabled (*e.g.*, Pd-NZVI based) site remediation, a comprehensive understanding of nanoparticle behavior in environmentally relevant media is necessary. In this study, we examine the impact of the deposited Pd-NZVI on biofilm viability and show direct evidence of Pd-NZVI deposition in/within the biofilm. Furthermore, several surface modifiers have been proposed to stabilize Pd-NZVI suspension with varied levels of success, and it is of interest to investigate the effect of the surface coatings during transport of surface-modified Pd-NZVI in biofilm-laden granular matrices. Thus, we used rhamnolipid biosurfactant and carboxymethylcellulose (CMC) as Pd-NZVI stabilizing surface modifiers based on their effectiveness, as demonstrated in our previous work.[7] These two anionic surface modifiers have very different molar masses, which will provide insight into the role of how the molecular size of the modifiers affects biofilm interactions.

The purpose of this study is to systematically investigate (i) the influence of biofilm coatings present on quartz sand on the transport behavior of surface-modified Pd-NZVI, and (ii) the impact of Pd-NZVI on the viability of the biofilm bacteria. *Pseudomonas aeruginosa* was chosen as a model biofilm forming bacterium as it is known to grow in both aerobic and anaerobic environments. To directly evaluate the influence of the biofilm, transport studies were conducted using columns packed with clean or biofilm-laden sand. The experiments were conducted over a wide range of ionic strengths using both monovalent (NaCl) and divalent ($CaCl_2$) salts. The distribution of Pd-NZVI on biofilm-coated sand was mapped using enhanced darkfield hyperspectral imaging and its potential impact on the microbial community was examined using standard viability assays.

Materials and methods

Pd-NZVI suspension

Bare NZVI particles were obtained from Golder Associates (Montreal, Canada). Palladization and surface modification were carried out in the laboratory, as previously described.[7] Based on the effectiveness demonstrated in our previous study,[7] two surface modifiers were chosen as Pd-NZVI stabilizing agents: (i) sodium-CMC (Sigma) with a molar mass ~700 kDa and (ii) rhamnolipid (RL) biosurfactant (JBR215, Jeneil Biosurfactant Co., Saukville, Wisconsin) with an average molar mass ~577 Da. The final suspension used in characterization and transport experiments contained 150 mg L^{-1} Pd-NZVI and 100 mg total organic carbon (TOC) per L surface modifier. The primary particle size based on transmission electron microscopy (TEM) was $<$100 nm.[23] The particle aggregates in the final suspension had a hydrodynamic diameter $>$100 nm, (Table S2†). Methods for the nanoparticle size (measured using dynamic light scattering) and electrophoretic mobility (measured using laser Doppler electrophoresis) characterization are described in the ESI.†

Granular medium and biofilm growth

Quartz sand (50–70 mesh, Sigma) with an average size of 256 μm (uniformity coefficient of 1.4 (ref. 20)) was used as a granular material for preparation of the packed columns. The sand was acid washed and baked at 800 °C as per the sand washing procedure described previously.[24,25] The biofilm growth protocol was adapted from our earlier work.[14] Briefly, *P. aeruginosa* PAO1 (ATCC# BAA-47) was selected as a model biofilm forming bacterium. Prior to growing biofilm, each batch of dry sand (27 g sand in 250 mL glass bottle) was autoclaved for 30 min. Next, 15 mL sterile LB (Lysogeny Broth) medium was added into the bottle followed by aseptic inoculation from a culture plate. The working culture plates were periodically prepared (once a week) from the stock pure culture (*P. aeruginosa*) stored at −80 °C. Finally, the biofilm was grown by incubating the mixture of sand and bacterial culture (in the glass bottle) at 37 °C for 24 hours with orbital shaking at 100 rpm.

Biofilm characterization by confocal microscopy

The biofilm-coated sand surface was characterized using confocal laser scanning microscopy (CLSM, Zeiss LSM 510 META). Two sets of confocal images were acquired: (i) after 24 h biofilm growth using sand grains collected from the top and bottom of the batch in the glass bottle used for growth, and (ii) from two segments (top and bottom) of the column packed with biofilm-coated sand after ~10 pore volumes (PVs) equilibration with either 10 mM NaCl or 10 mM $CaCl_2$. The biofilm staining protocol was adapted from our previous work.[14] Briefly, prior to imaging, the collected sand grains were placed on a microscope slide and stained with (i) Film Tracer FM 1-43 green biofilm cell stain (Life Technologies), and (ii) Film Tracer SYPRO Ruby Biofilm Matrix Stain (Invitrogen) for 15 min in the dark. After rinsing with DI water, the grains were then transferred into a bead of glycerol on a glass cover slip, and the confocal imaging (slicing with *z*-stack) was immediately started. The average biofilm thickness on the sand grains was determined by analyzing the images using Zen software as described previously.[14]

Biomass along the column

The distribution of biofilm along the sand-packed column was determined by gravimetric analysis as described elsewhere.[16] Briefly, the biofilm-coated sand matrix was dissected into four segments collected in separate ceramic cups. These cups were then dried at 120 °C for 14 h, cooled to room temperature, and weighed. To remove organic mass, the samples were then combusted at 800 °C for 24 h, cooled to room temperature, and re-weighed. The difference in mass represents the amount of biomass present in each column section. The distribution of biomass along the length of the biofilm-coated sand column after equilibration, but prior to Pd-NZVI injection, is presented in Fig. S1.†

Pd-NZVI transport experiments

Clean sand-packed column experiments were conducted as described previously.[7] Briefly, a glass column (GE Life Science – C16/20 tube (i.d. 1.6 cm) with AC 16 adapter) was wet packed with 27 g sand that was pre-equilibrated overnight with the electrolyte of interest. The packed bed length was 8.1 cm. Next, the column was equilibrated with the electrolyte of interest for ~10 PVs at a flow rate of 0.9 mL min^{-1} (approach velocity of 7.5×10^{-5} m s^{-1}) in downward flow direction using a peristaltic pump (ISMATEC, Model ISM596D). The Pd-NZVI suspension (either RL- or CMC-coated) was then injected at the same flow rate and direction using the same pump. Nearly 3 PVs of Pd-NZVI suspension (prepared in the background electrolyte of interest) was injected followed by the flushing phase with ~4 PVs background electrolyte to ensure complete removal of mobile Pd-NZVI from the column pore space. The concentration of Pd-NZVI in the influent (C_0) and effluent (C) suspensions was monitored (at 10 s intervals) online at 508 nm using a UV-vis spectrophotometer (Agilent 8453) equipped with a flow-through cell (1 cm path length).[7]

To ensure homogeneity and a constant injection concentration, the glass vial containing the Pd-NZVI suspension was continuously shaken at 400 rpm (INFORS HT Labotron bench-scale orbital shaker) throughout the experiment. Biofilm-coated sand column experiments were conducted in the same manner as the clean sand columns, with the exception that the sand was pre-coated with *P. aeruginosa* biofilm as described above. The equilibration, Pd-NZVI injection and post-injection procedures were the same as in the clean sand packed column experiments. Prior to conducting the nanoparticle transport experiment, the breakthrough behavior of an inert tracer (10 mM KNO_3) was monitored (Fig. S2†). All column experiments were conducted at least in duplicate, the range of elution in duplicate runs is reported in Table S4.†

Enhanced darkfield hyperspectral imaging

The presence of Pd-NZVI on biofilm-laden sand was detected and a qualitative spatial distribution confirmed using an enhanced darkfield transmission optical microscope (Olympus BX43) equipped with a hyperspectral imaging spectrophotometer (CytoViva, Inc., Auburn, AL). Grains of biofilm-coated sand (pre-exposed to Pd-NZVI suspension) were transferred to a glycerol bead on a glass slide and covered with a glass cover slip before capturing hyperspectral images. At least three hyperspectral images were collected for each treatment (biofilm-coated sand) exposed to either RL-coated or CMC-coated Pd-NZVI; treatments with no particle exposure served as a control (blank). To build the reference spectra library for analysis, hyperspectral images of the nanoparticle suspensions were also captured. The images were processed and analyzed using a hyperspectral imaging system software (ENVI 4.8 version). The heterogeneity of the Pd-NZVI suspension was accounted for by randomly selecting several particles (regions of interest) to build the spectral library. The spectral library was then filtered through the blank to eliminate matching profiles. Analysis was subsequently performed using the modified spectral library and a spectral angle mapping (SAM) coefficient of 0.08 to spectrally determine the spatial distribution of the nanoparticles.

P. aeruginosa growth in the presence or absence of Pd-NZVI

The potential influence of the Pd-NZVI during bacterial growth and biofilm formation was investigated. An overnight culture was grown in LB at 37 °C (for 20 hours) with shaking at 130 rpm. The bacterial culture was then diluted 100 times (to an optical density at 600 nm, OD_{600}, between 0.04–0.05) and distributed (900 μL aliquots) into a 24-well black microplate with clear bottom (PerkinElmer). Each well was loaded with 100 μL Pd-NZVI suspension from the stock prepared at two different Pd-NZVI concentrations (1.5 and 0.15 g L^{-1}) that resulted in final Pd-NZVI concentrations of 0.15 or 0.015 g L^{-1}. Selected wells without Pd-NZVI served as controls. To distinguish the effect of particle modifier, additional

experiments were conducted using the supernatant of the Pd-NZVI suspension containing free (unbound) surface modifiers. The Pd-NZVI was first separated from the unbound surface modifiers using a super magnet. The plates were incubated in a microplate reader (Tecan Infinite M200 Pro, Switzerland) at 37 °C with orbital shaking (1000 s, 1.5 mm amplitudes, wait time 1 min) and the planktonic growth (OD_{600}) monitored at 30 min intervals for 24 h. All experiments were conducted in triplicate.

Effect of Pd-NZVI on biofilm development

At the end of the 24 h growth period described above, the liquid (non-adherent cells) in each well was removed by gentle pipetting. The wells were then washed two times with deionized (DI) water and stained with 0.1% crystal violet (CV) (1 mL per well). After 15 min, the excess CV stain was removed, the wells were rinsed three times with DI water, and the CV was solubilized with 95% ethanol (1 mL per well) for 15 min. Finally, OD_{570} values in each well were measured using the microplate reader and reported as the quantitative measure of biofilm formed. To account for the variations in growth, biofilm level (OD_{570}) was normalized by the level of bacterial growth (OD_{600}) at the end of growth period (24 h).

Bacterial viability assay

Overnight cultures, diluted 100 times, were loaded into 24-well plates (1 mL per well) that were incubated at 37 °C for 24 h with orbital shaking at 100 rpm. After 24 h, the non-adherent cells in each well were removed by gentle pipetting. The thin layer of biofilm formed on the well surfaces was then exposed to 15 or 150 mg L^{-1} RL-coated or CMC-coated Pd-NZVI suspension (1 mL per well) prepared in 10 mM NaCl. To avoid Pd-NZVI oxidation during exposure, the plates were kept in an anaerobic chamber at room temperature. At the end of exposure period (1 or 24 h), the suspension in each well was removed by gentle pipetting followed by

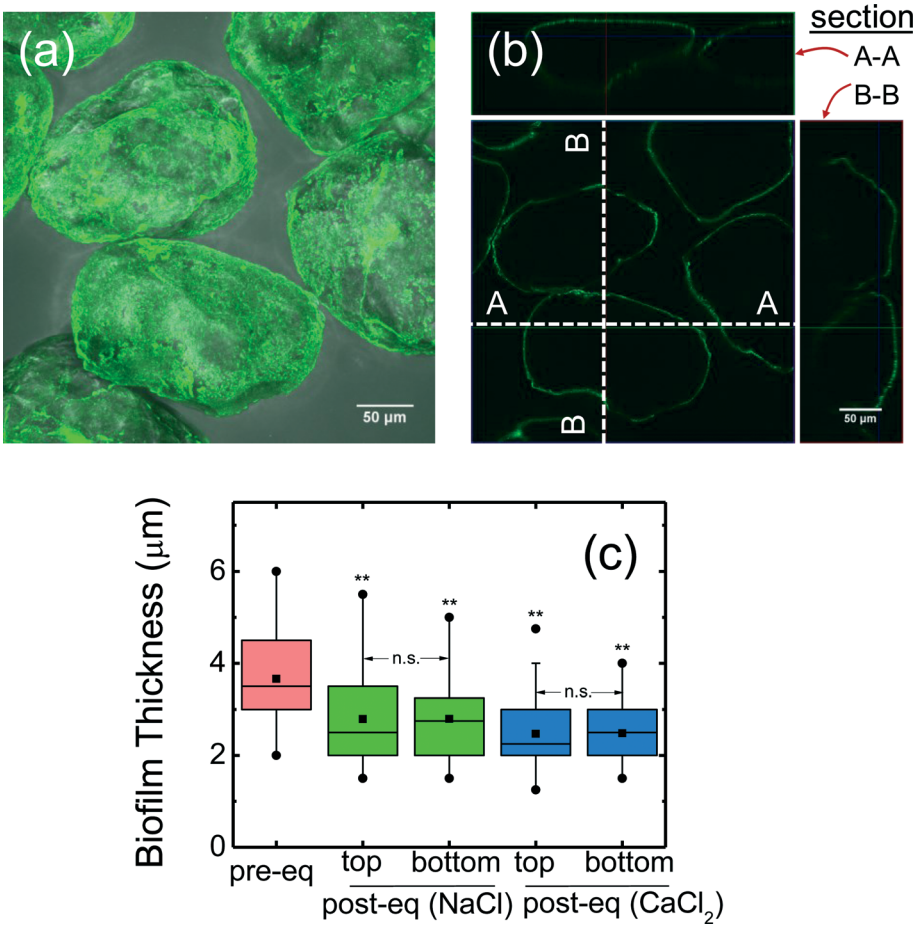

Fig. 1 (a) Confocal micrograph of quartz sand coated with *P. aeruginosa* biofilm (overlay of dark field and Film Tracer™ Green Biofilm Cell Stain). (b) Representative orthogonal confocal image of biofilm-coated sand grain showing biofilm thickness on the sand surface. Three images per treatment (with *z*-stacking) were acquired to measure biofilm thickness using the CLSM image processing software. (c) Biofilm thickness on the quartz sand surface before column packing (pre-eq) with the sample collected from the glass bottle in which the biofilm was grown, and after column packing and equilibration (post-eq) with either 10 mM NaCl or 10 mM $CaCl_2$. To collect sand grains for confocal imaging, the column was dissected into two segments (top and bottom) following the equilibration. The box plot is based on at least 60 independent thickness measurements per treatment. Statistically significant differences with respect to pre-equilibration is indicated by ** ($p < 0.01$, *t*-test) (n.s. – no significant difference).

staining with 200 μL per well of 1 : 1 mixture of Live/Dead stain (LIVE/DEAD® BacLight™ Bacterial Viability Kit, Life Technologies) for 15 min. The BacLight mixture consists of SYTO 9 and propidium iodide that stains cells with compromised membranes red and cells with intact membranes green. After 15 min contact time (in the dark), excess stains in the wells were removed, followed by imaging using fluorescence microscopy (IX-71, Olympus) at 200× magnification. At least 30 images were acquired per treatment, and analyzed using ImageJ (ImageJ 1.43 m, NIH, USA) to determine the total area of compromised (red) and uncompromised (green) cells. The loss in cell viability was calculated as the ratio of red to total (red + green) area.

Results and discussion

Biofilm thickness characterization

A representative confocal image of biofilm-coated sand is presented in Fig. 1a, which shows a homogeneous biofilm coating on the sand surface. An orthogonal confocal image shows a thin layer of biofilm around the sand (Fig. 1b). Measured biofilm thickness on the sand surface (after 24 hours growth) is shown in Fig. 1c. The thickness before column packing was 3.7 ± 0.17 μm (mean ± 95% confidence interval). After column packing and equilibration, the thickness decreased ($p < 0.05$, *t*-test) with the mean of the top (inlet end) and bottom (outlet end) values as 2.8 ± 0.15 μm and 2.5 ± 0.05 μm respectively for 10 mM NaCl and $CaCl_2$ equilibrated columns (Fig. 1c). During equilibration, some of the loose biofilm likely dislodged from the sand surface, resulting in slightly thinner biofilm observed after equilibration. Additionally, no apparent difference in biofilm thickness was observed between the top or bottom column segments ($p > 0.05$) suggesting a homogeneous biofilm distribution along the column. This result is consistent with a previous study[14] where the same biofilm forming approach was used, although the thickness reported was higher (~4 μm) than this study (2.5–2.8 μm). These differences may be attributed to the different quartz sand used (average grain size of 256 μm in this study *versus* 760 μm in the previous study[14]), likely leading to different packing arrangement and different surface roughness, and thus slightly different growth conditions. Owing to its smaller grain size, the available surface area for biofilm growth is much larger (3 times more for a given volume) in this study. Moreover, the approach velocity in this study (7.46×10^{-5} m s^{-1}) was higher than in the previous study (6.22×10^{-5} m s^{-1}).[14]

Electrokinetic characterization and hydrodynamic diameter of Pd-NZVI

For RL-coated Pd-NZVI, the EPM values varied from −4 to −2.5 μm cm V^{-1} s^{-1} in 3–100 mM NaCl, and −2 to −1 μm cm V^{-1} s^{-1} in 1–30 mM $CaCl_2$ (Fig. S3†). The EPM values for CMC-coated Pd-NZVI varied from −4.5 to −2.5 μm cm V^{-1} s^{-1} in NaCl and −4 to −1.5 μm cm V^{-1} s^{-1} in $CaCl_2$ (Fig. S3†). Overall, the EPM data shows that (i) in both monovalent and divalent salts, an increase in solution ionic strength results in lower absolute EPM values due to compression of the diffuse double layer and charge screening, (ii) at a given ionic strength, the divalent salt is more effective at masking the charge as noted by the significantly lower EPM values in $CaCl_2$ compared to NaCl.

The stability or the aggregation state of Pd-NZVI used in the transport experiments was assessed by measuring the hydrodynamic diameters of Pd-NZVI using dynamic light scattering (d_{DLS}) (Fig. S4 and Table S2,† influent d_{DLS}). Broadly, the sizing data correlates with the EPM data, *i.e.*, the extent of aggregation generally increased with the decreased absolute EPM (electrostatic destabilization). For RL-coated Pd-NZVI in NaCl, the average d_{DLS} value ranged from 402 ± 20 nm at 3 mM to 518 ± 20 nm at 30 mM (difference statistically significant, $p < 0.001$), whereas in $CaCl_2$ a larger d_{DLS} is observed over the same range of ionic strength (IS); the average d_{DLS} ranged from 700 ± 35 nm at 3 mM to 1590 ± 64 nm at 30 mM. Likewise, for CMC-coated Pd-NZVI in NaCl, the average d_{DLS} ranged from 435 ± 35 nm at 3 mM to 1510 ± 51 nm at 30 mM, whereas the particle size was considerably larger in $CaCl_2$: average d_{DLS} ranged from 2317 ± 132 nm at 3 mM to 2285 ± 177 nm at 30 mM (Fig. S4 and Table S2,† influent d_{DLS}). It is worth noting that these values should be interpreted with caution as the DLS measurements may be biased by the sedimentation of larger aggregates present in the suspension.

Overall, the sizing data indicate that the extent of aggregation increases with IS. This result corroborates our previous work where an IS dependent aggregation behavior was demonstrated for both RL- and CMC-coated Pd-NZVI over a broad range of IS (10–500 mM $NaHCO_3$).[7] At a given IS, $CaCl_2$ is more effective at inducing agglomeration as depicted by larger d_{DLS} values in $CaCl_2$ (Fig. S4†). The presence of Ca^{2+} notably reduces the absolute EPM of Pd-NZVI (due to charge screening) resulting in reduced particle–particle repulsive interaction which favors aggregation. Moreover, Ca^{2+}-induced bridging mechanism between the carboxylic group containing coating molecules of Pd-NZVI can lead to further aggregation. This result is consistent with a prior study that reported increased NZVI aggregation in the presence of $CaCl_2$.[26]

Transport of Pd-NZVI suspended in monovalent salt solution

The results of Pd-NZVI transport experiments in biofilm-coated sand in the presence of monovalent salt (NaCl) are presented in Fig. S5 and Table S4.† For RL-coated Pd-NZVI, particle elution (C/C_0) systematically decreases with an increase in IS; the average C/C_0 varies from 0.80 at 3 mM to 0.12 at 100 mM NaCl (Table S4†). For CMC-coated Pd-NZVI, although the elution does vary slightly from 3–10 mM (C/C_0 = 0.85–0.86), a drastic reduction in elution occurs at 30 mM (C/C_0 = 0.28) and 100 mM (C/C_0 = 0.18) (Table S4†). The elution in biofilm-coated sand is compared to experiments

conducted in clean sand from our previous study,[23] in which the same sand was used. Overall, at a given IS, reduced elution is observed in biofilm-coated sand compared to clean sand (*i.e.*, $C/C_{0,\text{biofilm}} < C/C_{0,\text{clean}}$), except for one treatment (CMC-coated Pd-NZVI at 10 mM NaCl) (Table S4†). To be more representative of field conditions, additional experiments conducted at higher Pd-NZVI concentration (1 g L^{-1}) show that RL and CMC are effective at improving Pd-NZVI transport even in biofilm-coated sand (C/C_0 = 0.60 ± 0.02 for RL-coated and 0.77 ± 0.01 for CMC-coated Pd-NZVI) (Fig. S6a†).

A semi-quantitative comparison of nanoparticle transport potential is made *via* the calculated attachment efficiency (α_{pc})[27,28] (Fig. 2). The α_{pc} values for columns packed with clean sand were obtained from our previous work.[23] Overall, in both treatments, the α_{pc} values increase with an increase in solution IS (Fig. 2a and b). As explained in the section on electrokinetic characterization, an increase in solution IS results in lower absolute EPM and thus reduced repulsive electrostatic forces that favor the likelihood of particle attachment onto the collector surfaces. Another important observation is that, at a given IS, the biofilm-coated sand results in greater α_{pc} values. For RL-coated Pd-NZVI, we observe 2 to 6 fold increase in α_{pc} in biofilm-coated sand *versus* bare sand; the increase is ~2 fold for CMC-coated Pd-NZVI (Fig. 2a and b). Likewise, at 1 g L^{-1} Pd-NZVI, a 1.6 fold (RL-coated) to 16 fold (CMC-coated) increase in α_{pc} is observed in biofilm-coated sand (Fig. S6b†). The implication of these calculations is that the transport potential of these nanoparticles is potentially reduced in granular groundwater environments that contain biofilm. Therefore, (Pd-) NZVI transport studies conducted in clean sand may overestimate the transport potential of these reactive nanoparticles in natural environments. Lerner *et al.*[17] also reported a larger α_{pc} value for the transport of poly(acrylic) acid-stabilized NZVI in columns packed with biofilm-coated glass beads (α_{pc} = 0.03) *versus* clean glass beads (α_{pc} = 0.004) at 25 mM NaCl.[17] However, the difference in α_{pc} was negligible at 1 mM NaCl (α_{pc} = 0.006 and 0.005, respectively, in clean and biofilm-coated media).

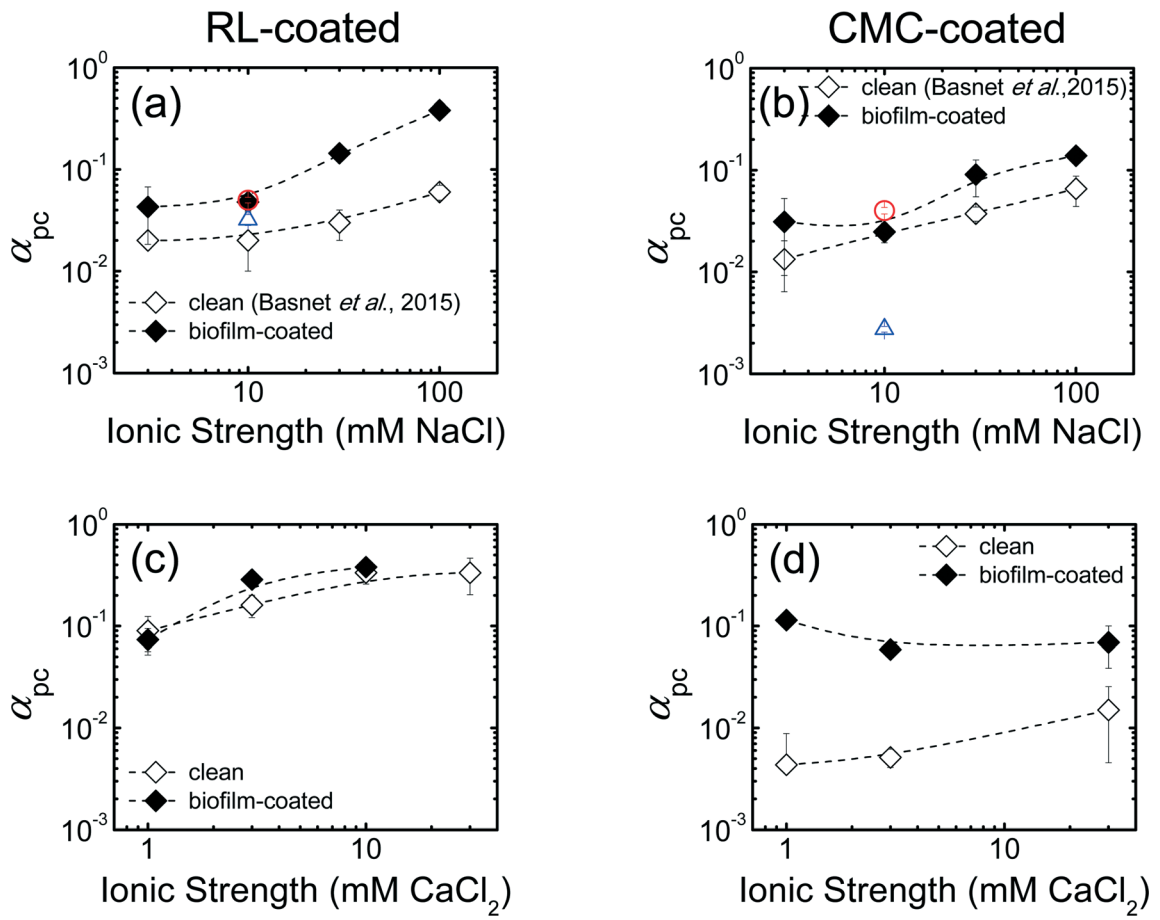

Fig. 2 Calculated particle-collector attachment efficiency (α_{pc}) in monovalent salt (NaCl) for (a) RL-coated and (b) CMC-coated Pd-NZVI in clean and biofilm-coated sand column. The α_{pc} values in clean sand were adopted from our previous work.[23] The α_{pc} values in divalent salt ($CaCl_2$) for (c) RL-coated and (d) CMC-coated Pd-NZVI in clean and biofilm-coated sand columns. Error bars represent standard deviations. The dashed lines are included to guide the eye. The circular red and triangular blue symbols on Fig. 2a and b correspond to the transport experiment conducted at higher Pd-NZVI concentration (1 g L^{-1}) in biofilm coated-sand and clean sand (from our previous work[23]), respectively. For all other conditions, the particle concentration was 0.15 g L^{-1}.

To determine whether larger aggregates were preferentially retained within the column matrix, hydrodynamic diameter (d_{DLS}) of Pd-NZVI were measured for both influent and effluent suspensions (Table S2†). At lower IS (up to 10 mM NaCl), both influent and effluent d_{DLS} were comparable for both RL- and CMC-coated Pd-NZVI. However, at higher IS (*e.g.* 100 mM NaCl), effluent d_{DLS} (437 ± 21 nm for RL-coated, 591 ± 107 nm for CMC-coated) were significantly smaller than influent d_{DLS} (634 ± 25 nm for RL-coated Pd-NZVI and 1350 ± 155 nm for CMC-coated Pd-NZVI), which suggests preferential retention of larger aggregates in the granular medium.

Transport of Pd-NZVI suspended in divalent salt solution

The results of Pd-NZVI transport experiments in clean and biofilm-coated sand in the presence of divalent salt ($CaCl_2$) are presented in Fig. S7 and Table S4.† For RL-coated Pd-NZVI, both in clean and biofilm-coated sand, Pd-NZVI transport systematically decreases with IS. In clean sand, the average breakthrough elution (C/C_0) varies from 0.62 at 1 mM to 0.01 at 30 mM, whereas in biofilm-coated sand, C/C_0 varies from 0.67 at 1 mM to 0.06 at 10 mM. Overall, nanoparticle elution is reduced in biofilm-coated sand compared to clean sand, except at 1 mM. For CMC-coated Pd-NZVI, in clean sand, the extent of nanoparticle elution decreases with an increase in IS; C/C_0 varies from 0.93 at 1 mM to 0.65 at 30 mM. The elution decreases more significantly in biofilm-coated sand (C/C_0 ~ 0.15) at all the IS investigated (1–30 mM $CaCl_2$) (Fig. S7d†). It is important to note that high concentrations of calcium ions (>10 mM) are less common in groundwater environments, and the high concentrations were chosen here for a direct comparison with NaCl.

Based on the C/C_0 values presented in Table S4,† it is evident that at a given IS, divalent salt ($CaCl_2$) results in enhanced deposition (*i.e.*, reduced elution) than monovalent salt (NaCl) in both clean and biofilm-coated sand. There are three possible contributing factors for this observation. First, the presence of Ca^{2+} notably reduces the absolute EPM of the Pd-NZVI (Fig. S3†) and the zeta potential of the clean or biofilm-coated sand[14] resulting in reduced particle-collector repulsive interactions and thus favoring Pd-NZVI deposition. Second, the significant aggregation observed in the presence of $CaCl_2$ (Fig. S4†) would lead to preferential retention of larger aggregates. Third, analogous to particle–particle aggregation caused by bridging of COOH-containing coating molecules, the presence of calcium ion may contribute to bridging with the functional groups within the EPS in biofilm matrices (and thus increased deposition).

The results of column transport experiments for Pd-NZVI suspended in $CaCl_2$ can be compared semi-quantitatively using α_{pc} values (Fig. 2c and d). For RL-coated Pd-NZVI, in clean sand, the α_{pc} value increases from 0.09 at 1 mM to 0.33 at 10 mM. A similar trend is observed in biofilm-coated sand; α_{pc} varies from 0.07 at 1 mM to 0.38 at 10 mM. For this treatment, the effect of biofilm to reduce Pd-NZVI transport potential is evident at 3 mM ($\alpha_{pc,biofilm} > \alpha_{pc,clean}$, $p < 0.05$) but not at 1 and 10 mM $CaCl_2$ (Fig. 2c). For CMC-coated Pd-NZVI, in clean sand, α_{pc} increases from 0.004 at 1 mM to 0.02 at 30 mM. In contrast, there is no significant change in α_{pc} for CMC-coated Pd-NZVI in biofilm-coated sand. Overall, the most important observation from Fig. 2d is that α_{pc} is significantly higher in the presence of biofilm (5 to 26 fold increase in α_{pc} values in the presence of biofilm).

In $CaCl_2$, considerable differences in influent and effluent d_{DLS} were noted (Table S2†), likely due to enhanced aggregation of the influent suspension (Fig. S4†) and preferential retention of larger aggregates during transport. For example, for RL-coated Pd-NZVI at 10 mM $CaCl_2$, the effluent d_{DLS} (542 ± 17 nm in clean sand and 364 ± 26 nm in biofilm-coated sand) is smaller than influent d_{DLS} (906 ± 36 nm). For CMC-coated Pd-NZVI at 30 mM $CaCl_2$, the effluent d_{DLS} (1424 ± 108 nm in clean sand and 1012 ± 171 nm in biofilm-coated sand) is smaller than influent d_{DLS} (2285 ± 177 nm) (Table S2†). Smaller effluent d_{DLS} in biofilm-coated sand than in clean sand is an indication that the biofilm may act as collector of larger aggregates, *i.e.*, physical straining is likely an important mechanism for the retention of Pd-NZVI aggregates in the presence of biofilm.

Characterization of biofilm-coated sand using hyperspectral imaging

The presence of Pd-NZVI on the biofilm-coated sand surface is confirmed *via* enhanced darkfield hyperspectral imaging and spectral mapping (red dots in images – Fig. 3a and b). RL- and CMC-coated Pd-NZVI exhibit unique spectral profiles (Fig. 3c and d, respectively) that allows for their detection on the biofilm-coated surface. The average peak wavelength is ~625 nm and ~575 nm for RL-coated Pd-NZVI and CMC-coated Pd-NZVI, respectively. The biofilm-coated sand also exhibits a distinct spectral profile with average peak values at significantly higher wavelengths (average ~775 nm) (Fig. 3e and f) compared to the Pd-NZVI. Moreover, hyperspectral images of bare and coated Pd-NZVI suspensions (Fig. S8†) indicate the stabilizing effect of the surface modifiers; we note aggregated clusters of bare Pd-NZVI compared to RL- and CMC-coated Pd-NZVI. This is the first study to characterize Pd-NZVI deposited on biofilm-coated sand grains using hyperspectral imaging. Enhanced darkfield microscopy based hyperspectral imagery can be a promising tool to detect, characterize and semi-quantify nanoparticles in complex environmental matrices, and thus better enable understanding of their fate and transformation.[29] However, challenges occur when attempting to distinguish nanoparticles from the environmental matrices (*e.g.*, aquifer grains) when the former and latter have similar spectral profiles. Furthermore, identification of nanoparticles is influenced by changes to their spectral profiles that can occur due to adsorption or surface complexation of natural organic matter.

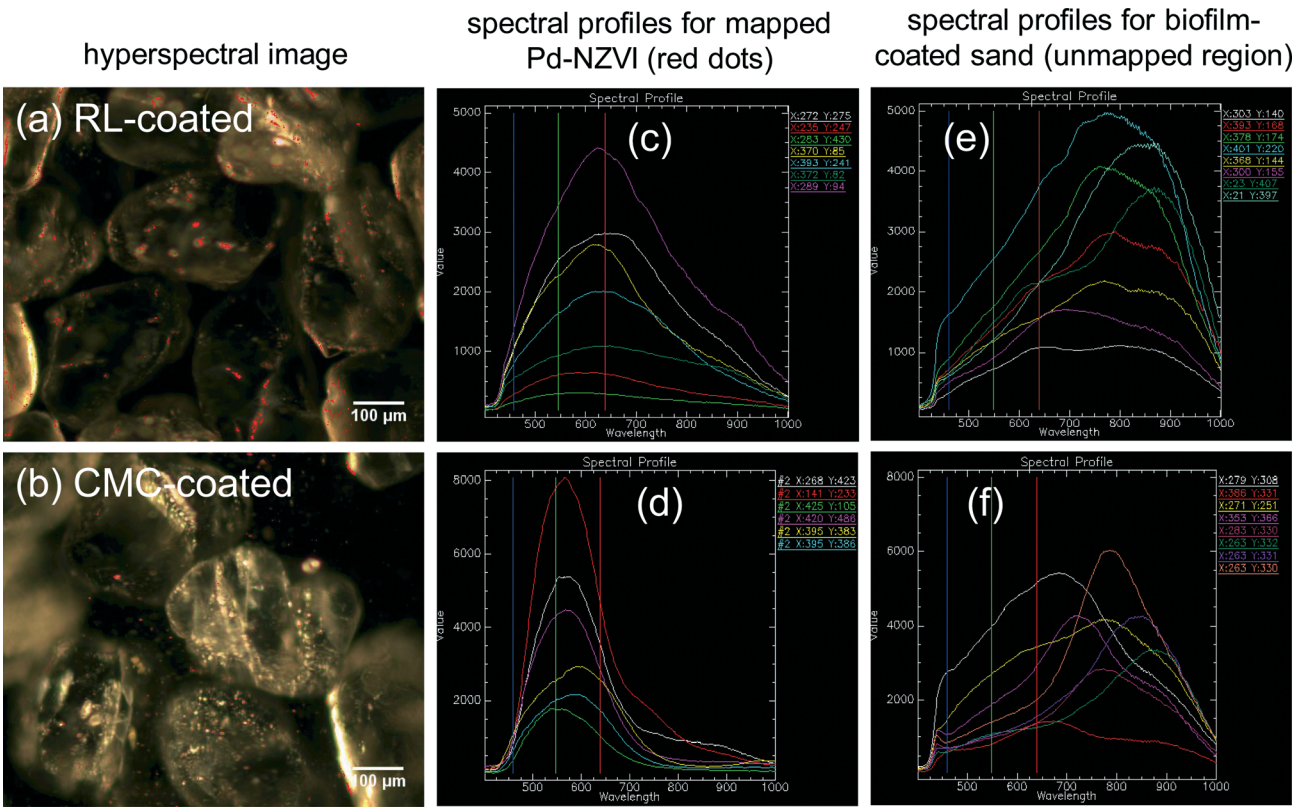

Fig. 3 Hyperspectral images of biofilm-coated sand exposed with (a) RL-coated and (b) CMC-coated Pd-NZVI. Red dots represent mapped Pd-NZVI particles on the biofilm matrices. The representative spectral profiles correspond to the mapped (c) RL-coated and (d) CMC-coated Pd-NZVI. The representative spectral profiles for the unmapped region (biofilm-coated sand only) are also presented (e, f).

Effect of coated Pd-NZVI on *P. aeruginosa* growth

Bacterial growth curves in the absence or presence of Pd-NZVI are presented in Fig. 4a and b. Growth kinetics are stimulated (higher OD_{600} values) at lower Pd-NZVI concentration (15 mg L^{-1}) for both RL- and CMC-coated Pd-NZVI. The presence of small amount of iron and/or the associated surface modifiers appear to favor the bacterial growth. In contrast, a markedly inhibited growth rate is observed at higher Pd-NZVI concentration (150 mg L^{-1}). Murugesan *et al.*[30] also reported a comparable trend whereby the bacterium (*Sphingomonas* sp. PH-07) was able to grow well at lower Pd-NZVI concentration (<0.1 g L^{-1}) at 25 °C. However, an inhibited bacterial growth was observed when Pd-NZVI concentration was greater than 0.1 g L^{-1}.[30] Based on our previous work[7] a notable fraction (>80%) of free surface modifier is likely to remain in the suspension; therefore to elucidate its effect, additional growth experiments were conducted in the presence of free (unbound) surface modifier. The supernatant of CMC- and RL-coated Pd-NZVI suspension was collected by separating the NZVI with a super magnet. The experiments show comparable growth as with the control (Fig. 4e and f), suggesting that the surface modifiers (RL and CMC) had no adverse effects on bacterial growth. For the bare Pd-NZVI, the growth was not affected at a lower concentration (15 mg L^{-1}), however, a marked inhibited bacterial growth was observed at a higher Pd-NZVI concentration (150 mg L^{-1}) (Fig. 4g). The presence of dissolved Fe during growth experiment cannot be ruled out, thus the inhibitory effect observed here might also be linked to the presence of dissolved ions. The toxicity of dissolved Fe^{2+} and Fe^{3+} ions to phytoplankton *P. subcapitata* has previously been reported.[26] Moreover, NZVI toxicity to *E. coli* has been associated with oxidative stress in the presence of released Fe ions due to oxidation.[31]

Effect of surface-modified Pd-NZVI on formation of *P. aeruginosa* biofilm

A quantitative estimate of biofilm formed over a 24 h growth period in the absence (control) or presence of RL- and CMC-coated Pd-NZVI (at 15 and 150 mg L^{-1}) is presented in Fig. 4c. Biofilm levels (OD_{570}) were normalized to the extent of bacterial growth (OD_{600}, determined separately) to decrease the potential bias in the measurements due to differences in growth rate.[32,33] Biofilm formation decreased in the presence of RL-coated Pd-NZVI, by 23% and 57% (compared to control) at 15 and 150 mg L^{-1}, respectively. For CMC-coated Pd-NZVI, biofilm formation was slightly decreased (by 3%) at 15 mg L^{-1} but increased (by 29%) at 150 mg L^{-1} (Fig. 4c). Biofilm formation was notably reduced in the presence of the unbound surface modifier (collected as supernatant of 150 mg L^{-1} RL- and CMC-coated Pd-NZVI

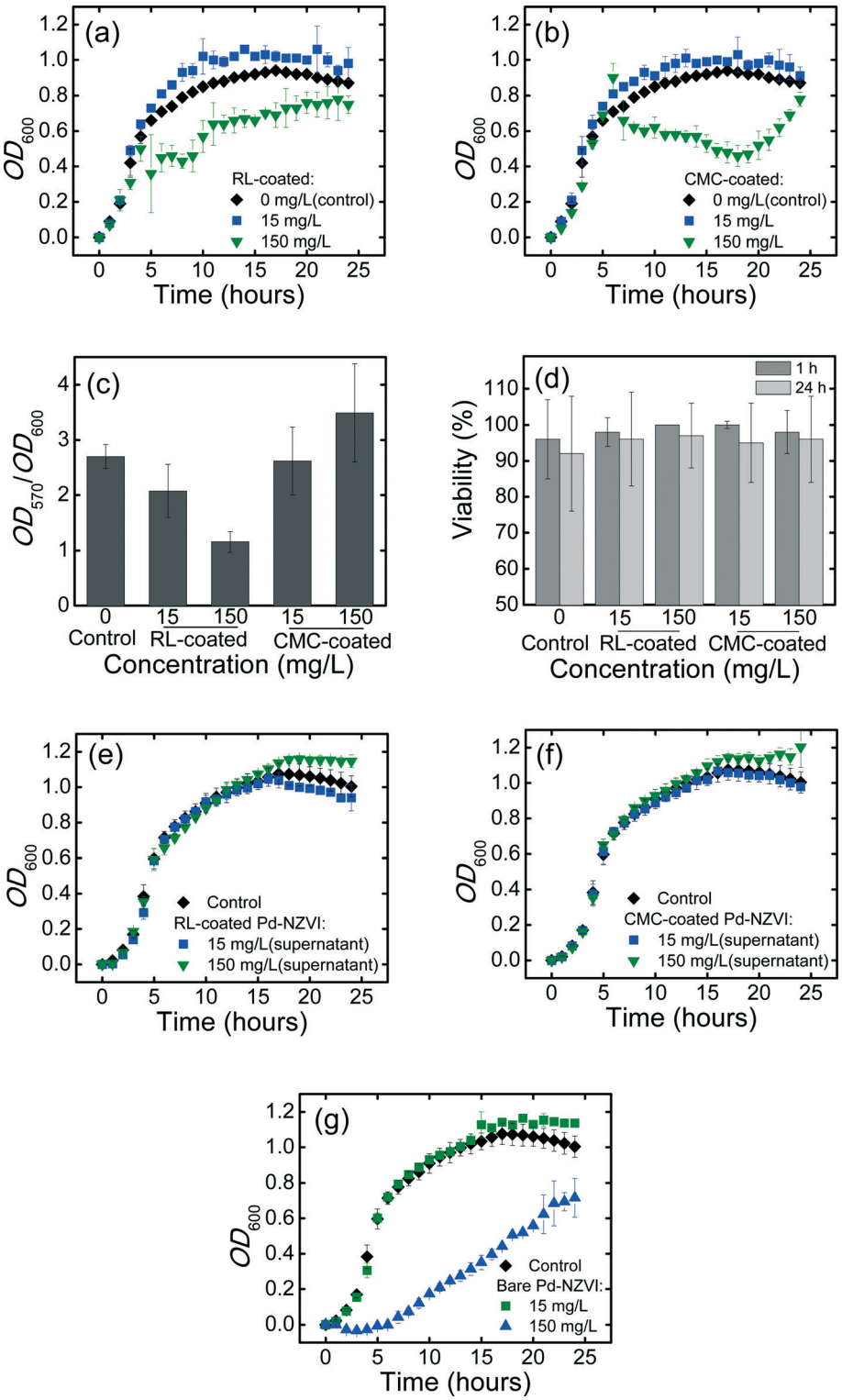

Fig. 4 (a, b) Bacterial growth curves measured as OD_{600} in the absence (control) or presence of (a) RL-coated and (b) CMC-coated Pd-NZVI at 15 and 150 mg L^{-1}. (c) Growth normalized quantitative estimate of the biofilm formed at the end of growth period (24 hours) measured using crystal violet assay (OD_{570}/OD_{600}). (d) Bacterial viability measured with LIVE/DEAD assay after 1 or 24 h exposure with Pd-NZVI at 15 and 150 mg L^{-1}. Error bars represent standard deviations. (e) Bacterial growth curves in the absence (control) or presence of free surface modifiers (supernatant) separated using super magnet for (e) RL-coated and (f) CMC-coated Pd-NZVI at 15 and 150 mg L^{-1}. (g) Bacterial growth curves in the absence (control) and presence of bare Pd-NZVI at 15 and 150 mg L^{-1}.

suspensions) and bare Pd-NZVI at both 15 and 150 mg L^{-1} (Fig. S9†). Therefore, biofilm inhibition appears to correlate with Pd-NZVI concentration at 150 mg L^{-1} with RL coating (both suspension and supernatant) and with CMC coating (supernatant). Using a microtiter dish assay, Davey *et al.*[34] also reported reduced *P. aeruginosa* biofilm formation in the presence of rhamnolipid.

Effect of deposited Pd-NZVI on viability of biofilm cells

The viability of matured (24 h) biofilm cells after 1 h or 24 h exposure to CMC- or RL-coated Pd-NZVI is presented in Fig. 4d (representative Live/Dead fluorescence microscopy images are presented in Fig. S10†). At 15 mg L^{-1} Pd-NZVI, with 1 h exposure, the average viability >96%, and a similar high viability (>98%) was observed at 150 mg L^{-1}. Inspection of Fig. 4d indicates some loss of viability at 24 h; however, the effect is not statistically significant. Additional biofilm viability experiments conducted using 1 g L^{-1} coated Pd-NZVI and its supernatant (free surface modifier) did not indicate any loss in viability (Fig. S11†). Therefore, overall, the viability assay suggests that exposure to either RL- or CMC-coated Pd-NZVI does not impact the membrane integrity of biofilm cells. As described previously for aggregated silver nanoparticles,[35] the Pd-NZVI suspension likely aggregated during the exposure period, and it is likely that the aggregated clusters did not penetrate the matrix of extracellular polymeric substances (EPS) as readily, thus limiting their impact on cell viability.

Environmental implications

This study highlights how the processes of nanoparticle aggregation and retention (by deposition and physical straining) are of importance in determining the suitability of NZVI-based remediation in field application, in the presence of natural biofilms. It is important to note that injection of large quantities of NZVI suspension likely displaces natural groundwater, especially near the injection point and may alter the influence of the natural water chemistry. This work shows that the transport potential of RL and CMC-modified Pd-NZVI (at 150 mg L^{-1}) is drastically reduced in the presence of *P. aeruginosa* biofilm. We observe a marked increase in nanoparticle attachment efficiency in the presence of biofilm, indicating that surface-modified Pd-NZVI can exhibit decreased transport in biofilm-laden groundwater environment. As expected, the variation in water chemistries influenced Pd-NZVI aggregation behavior, with drastic aggregation occurring in the presence of divalent salt. Particle retention was particularly significant (C/C_0 ~ 0.15) for a markedly aggregated suspension (CMC-coated Pd-NZVI in divalent salt) in biofilm-coated sand. Transport experiments conducted at higher Pd-NZVI concentration (1 g L^{-1}) showed that RL and CMC are effective for improving Pd-NZVI transport even in biofilm-coated sand but with a reduced transport potential when compared to clean sand. An important observation is the difference in measured particle size at the column effluent and influent that confirmed the contribution of physical straining of large aggregates as an important mechanism for the heightened Pd-NZVI retention in biofilm-coated column. This phenomenon was enhanced at higher IS that induced substantial aggregation and leads to the conclusion that physical straining is expected to be an important mechanism during field injection. Another key contribution of this study is the use of hyperspectral imaging to confirm the presence of Pd-NZVI in complex biofilm-laden matrices. This technique may be relevant in field application to directly characterize unlabeled samples (solid and liquid) collected from the field and confirm the presence of injected nanoparticles.

This study shows that the toxicological impact of Pd-NZVI on bacteria varies if the latter is in a planktonic or a sessile state; the surface modifiers (RL and CMC) alone are non-toxic to the bacterial cells. Although the planktonic growth data indicate inhibitory effect at higher concentration (150 mg L^{-1}) for both bare and coated (RL- and CMC-) Pd-NZVI, biofilm formation was only impacted by RL-coated Pd-NZVI. However, viability staining suggests negligible impact of the deposited surface-modified Pd-NZVI onto matured biofilm matrices (viability >95%) for both RL- and CMC-coated Pd-NZVI. Given that the injected surface-modified Pd-NZVI nanoparticles for remediation application are likely to be retained more in the presence of biofilm, a systematic study on the prolonged exposure of biofilms to the reactive nanoparticles coupled with nanoparticle aging/oxidation is of interest for further study.

Acknowledgements

This research was supported by NSERC Strategic Grant 365253 and NSERC Discovery, Golder Associates Ltd., FQRNT, a MEDA to M. B., and the CRC program. A. G. was supported by a McGill SURE award. We thank M. Mitzel for assistance with confocal microscopy and E. Nadezhina (U. Montreal) for assistance with hyperspectral imaging.

References

1 W. Yan, A. A. Herzing, X.-Q. Li, C. J. Kiely and W. X. Zhang, *Environ. Sci. Technol.*, 2010, **44**, 4288–4294.
2 W. X. Zhang, *J. Nanopart. Res.*, 2003, **5**, 323–332.
3 W. X. Zhang, C.-B. Wang and H.-L. Lien, *Catal. Today*, 1998, **40**, 387–395.
4 P. G. Tratnyek and R. L. Johnson, *Nano Today*, 2006, **1**, 44–48.
5 N. Saleh, H.-J. Kim, T. Phenrat, K. Matyjaszewski, R. D. Tilton and G. V. Lowry, *Environ. Sci. Technol.*, 2008, **42**, 3349–3355.
6 A. Tiraferri and R. Sethi, *J. Nanopart. Res.*, 2009, **11**, 635–645.
7 M. Basnet, S. Ghoshal and N. Tufenkji, *Environ. Sci. Technol.*, 2013, **47**, 13355–13364.
8 T. Raychoudhury, N. Tufenkji and S. Ghoshal, *Water Res.*, 2012, **46**, 1735–1744.

9 C. M. Kocur, D. M. O'Carroll and B. E. Sleep, *J. Contam. Hydrol.*, 2013, **145**, 17–25.
10 E. D. Vecchia, M. Luna and R. Sethi, *Environ. Sci. Technol.*, 2009, **43**, 8942–8947.
11 R. L. Johnson, G. O. B. Johnson, J. T. Nurmi and P. G. Tratnyek, *Environ. Sci. Technol.*, 2009, **43**, 5455–5460.
12 X. Jiang, X. Wang, M. Tong and H. Kim, *Environ. Pollut.*, 2013, **174**, 38–49.
13 Z. Li, A. A. Hassan, E. Sahle-Demessie and G. A. Sorial, *Water Res.*, 2013, **47**, 6457–6466.
14 M. R. Mitzel and N. Tufenkji, *Environ. Sci. Technol.*, 2014, **48**, 2715–2723.
15 M. Tong, J. Ding, Y. Shen and P. Zhu, *Water Res.*, 2010, **44**, 1094–1103.
16 S. Tripathi, D. Champagne and N. Tufenkji, *Environ. Sci. Technol.*, 2012, **46**, 6942–6949.
17 R. N. Lerner, Q. Lu, H. Zeng and Y. Liu, *Water Res.*, 2012, **46**, 975–985.
18 Y. Xiao and M. R. Wiesner, *Environ. Sci. Technol.*, 2013, **47**, 2246–2253.
19 T.-O. Peulen and K. J. Wilkinson, *Environ. Sci. Technol.*, 2011, **45**, 3367–3373.
20 I. R. Quevedo and N. Tufenkji, *Environ. Sci. Technol.*, 2012, **46**, 4449–4457.
21 A. Tiraferri, K. L. Chen, R. Sethi and M. Elimelech, *J. Colloid Interface Sci.*, 2008, **324**, 71–79.
22 K. A. Huynh and K. L. Chen, *Environ. Sci. Technol.*, 2011, **45**, 5564–5571.
23 M. Basnet, C. D. Tommaso, S. Ghoshal and N. Tufenkji, *Water Res.*, 2015, **68**, 354–363.
24 A. J. Pelley and N. Tufenkji, *J. Colloid Interface Sci.*, 2008, **321**, 74–83.
25 G. M. Litton and T. M. Olson, *Environ. Sci. Technol.*, 1993, **27**, 185–193.
26 A. A. Keller, K. Garner, R. J. Miller and H. S. Lenihan, *PLoS One*, 2012, 7.
27 N. Tufenkji and M. Elimelech, *Environ. Sci. Technol.*, 2004, **38**, 529–536.
28 A. R. Petosa, D. P. Jaisi, I. R. Quevedo, M. Elimelech and N. Tufenkji, *Environ. Sci. Technol.*, 2010, **44**, 6532–6549.
29 A. R. Badireddy, M. R. Wiesner and J. Liu, *Environ. Sci. Technol.*, 2012, **46**, 10081–10088.
30 K. Murugesan, V. Bokare, J.-R. Jeon, E.-J. Kim, J.-H. Kim and Y.-S. Chang, *Bioresour. Technol.*, 2011, **102**, 6019–6025.
31 M. Auffan, W. Achouak, J. Rose, M.-A. Roncato, C. Chanéac, D. T. Waite, A. Masion, J. C. Woicik, M. R. Wiesner and J.-Y. Bottero, *Environ. Sci. Technol.*, 2008, **42**, 6730–6735.
32 D. H. Dusane, Z. Hosseinidoust, B. Asadishad and N. Tufenkji, *PLoS One*, 2014, 9.
33 Z. Hosseinidoust, N. Tufenkji and T. G. van de Ven, *Biofouling*, 2013, **29**, 457–468.
34 M. E. Davey, N. C. Caiazza and G. A. O'Toole, *J. Bacteriol.*, 2003, **185**, 1027–1036.
35 S. M. Wirth, G. V. Lowry and R. D. Tilton, *Environ. Sci. Technol.*, 2012, **46**, 12687–12696.